Journal of Histochemistry & Cytochemistry 2016, Vol. 64(6) 343–352

DOI: 10.1369/0022155416646089
jhc.sagepub.com
SAGE

Post-Irradiated Human Submandibular Glands Display High Collagen Deposition, Disorganized Cell Junctions, and an Increased Number of Adipocytes

Kihoon Nam, Christina L. Maruyama, Bryan G. Trump, Luke Buchmann, Jason P. Hunt, Marcus M. Monroe, and Olga J. Baker

School of Dentistry (KN, CLM, BGT, OJB) and Division of Otolaryngology, Department of Surgery (LB, JPH, MMM), University of Utah, Salt Lake City, Utah

Summary

Salivary glands are vital for maintaining oral health. Head and neck radiation therapy is one of the most common causes of salivary gland hypofunction. Little is known about the structural changes that occur in salivary glands after radiation therapy. The aim of this study is to understand the structural changes that occur in post-irradiated human (submandibular gland [SMG]) as compared with untreated ones. We determined changes in epithelial polarity, presence of collagen deposition, and alteration in adipose tissue. We used formalin-fixed paraffin-embedded human SMG from two female subjects exposed to head and neck irradiation. We utilized hematoxylin and eosin staining and Masson's Trichrome staining. The immunostained tissue sections were examined using confocal microscopy. The number and size of adipocytes per tissue section were calculated using ImageJ, Prism, and SPSS software. Post-irradiated human SMG displayed high collagen deposition, disorganized cell junctions, and an increased number of adipocytes as compared with non-irradiated controls. These findings are important to improve our understanding of the individual risk and variation in radiation-related salivary gland dysfunction. (J Histochem Cytochem 64:343–352, 2016)

Keywords

adipose, collagen, radiation, submandibular, tight junctions

Introduction

Head and neck cancer is a disease in which abnormal and uncontrolled cell division occurs in the tissues and organs around the head and neck, such as the gums, tongue, throat, sinuses, nose, and salivary glands.[1] According to the Cancer Facts & Figures 2015, approximately 3% of new cancer cases in the United States occur in the head and neck.[2] Despite recent technical advances in treatment, the 5-year survival rates of patients with head and neck cancer have not changed over the past five decades.[2,3] Multimodality therapy is common in head and neck cancer treatment, with frequent utilization of radiation.[4,5] During these treatments, patients are exposed to high-energy gamma rays, and they can experience several side effects, including nausea, vomiting, osteoradionecrosis, trismus, loss or alteration of taste, weight loss, and salivary gland dysfunction (resulting in dry mouth, caries, oral infections, and mucositis).[5,6] Specifically, dry mouth is a significant clinical concern because it can lead to oral infections, sleep disturbances, oral pain, and difficulty in chewing

Received for publication February 25, 2016; accepted April 1, 2016.

Supplementary material for this article is available on the *Journal of Histochemistry & Cytochemistry* Web site at http://jhc.sagepub.com/content/by/supplemental-data.

Corresponding Author:
Olga J. Baker, School of Dentistry, The University of Utah, 383 Colorow Dr., Room 289A, Salt Lake City, UT 84108-1201, USA.
E-mail: olga.baker@hsc.utah.edu

Journal of Histochemistry and Cytochemistry

Table 1. Patient Information.

Patient	Gender	Age	Treatment Dose (Gy)	Treatment Duration	SMG Collection (After IR)
1	Female	81	None	None	None
2	Male	81	None	None	None
3	Female	65	73.8	2 months	6 years 7 months
4	Female	39	70.2	2 months	6 months

Abbreviations: SMG = submandibular gland; IR = irradiated.

or swallowing food, all of which reduce the quality of life for many individuals.[7–9] Saliva stimulants, saliva substitutes, and oral moisturizers have been used to treat dry mouth, but they only provide temporary pain relief.[10,11] To develop new treatments, it is important to understand the effects of radiation on salivary glands.

Extensive investigations are underway to examine the effect of radiation on saliva secretion. In 1999, Henson et al. reported that saliva flow rate is reduced by ~50% to 60% with accompanying changes in saliva composition.[12] In addition, loss of acinar cells, glandular shrinkage, and radiation-induced oral mucositis have been reported.[13–15] More recently, Knox et al. reported that irradiated human salivary glands display reduced parasympathetic innervation.[16] However, the exact cause of salivary gland dysfunction after radiation is still unclear. The aim of this study is to understand the structural changes that occur in post-irradiated submandibular glands (SMGs) as compared with untreated ones. Specifically, we determined changes in epithelial polarity, presence of collagen deposition, and alteration in adipose tissue.

Materials and Methods

Materials

Formalin was purchased from Baker (Phillipsburg, NJ). Goat serum was purchased from Sigma-Aldrich (St. Louis, MO). Rabbit anti-zonula occludens-1 (ZO-1) antibody was purchased from Invitrogen (Carlsbad, CA). Mouse anti-E-cadherin antibody was purchased from BD Biosciences (San Jose, CA). Triton X-100, phosphate buffered saline (PBS), Alexa Fluor 488 conjugated goat anti-rabbit secondary antibody, Alexa Fluor 568 conjugated goat anti-mouse secondary antibody, Alexa Fluor 538 conjugated phalloidin, TO-PRO-3 iodide, and ProLong Gold antifade reagent were purchased from Thermo Fisher Scientific (Newington, NH).

Patients

Formalin-fixed, paraffin-embedded human SMGs from the subjects listed in Table 1 were obtained from the University of Utah, Department of Otolaryngology, Head and Neck Surgery. All human specimen usage was conducted under the strict guidelines and approval of the University of Utah Health Sciences Institutional Review Board, and informed consent was obtained for each patient. Head and neck irradiation causes structural alteration of SMGs. Our studies are consistent with previous studies showing structural alterations after irradiation. This is the first study to quantify the amount and distribution of adipocytes and collagen deposition after irradiation in humans. Furthermore, we showed tight junction alteration after irradiation. These findings are an important first step in improving our understanding of the individual risk and variation in radiation-related salivary gland dysfunction.

Paraffin-Embedded Tissue

SMGs from irradiated and non-irradiated head and neck cancer patients were fixed in 10% formalin for 24 hr at room temperature. Paraffin-embedded, 5-µm sections were prepared at the ARUP Laboratories (Salt Lake City, UT). Formalin-fixed, paraffin-embedded SMG slides were deparaffinized by washing three times for 5 min in 100% xylene. Slides were washed for 5 min in xylene:ethanol (1:1), twice for 5 min in 100% ethanol, followed by 5 min washes in 95%, 80%, 70%, and 50% ethanol and twice in distilled water, respectively.

Hematoxylin and Eosin Staining

The rehydrated slides were stained with Harris Hematoxylin for 6 min and washed for 2 min with distilled water, 1 min with 0.5% lithium carbonate (Li_2CO_3; w/v), and 1 min with distilled water. Slides were washed for 1 min with 95% ethanol, followed by a 1-min incubation with Eosin and washed for 1 min with 95% ethanol. Finally, sections were washed three times with 100% ethanol, cleared in xylene, and mounted with a xylene-based mounting medium. The samples were examined using a Leica DMI6000B

inverted microscope (Leica Microsystems, Wetzlar, Germany).

Masson's Trichrome Staining

The rehydrated slides were re-fixed in Bouin's solution at 60C for 1 hr. Slides were rinsed in running tap water for 10 min to remove yellow color from sections. Then, slides were washed with distilled water for 5 min. For nuclei staining, slides were stained in Weigert's iron hematoxylin solution for 10 min, rinsed with running warm tap water for 10 min, and washed with distilled water for 5 min. For cytoplasm staining, slides were incubated in Biebrich scarlet-acid fuchsin solution for 5 min and washed three times with distilled water for 2 min. For collagen staining, slides were incubated in phosphotungstic/phosphomolybdic acid for 15 min, transferred directly to aniline blue solution, stained for 5 min, and washed three times with distilled water for 2 min. Then, sections were differentiated in 1% acetic acid solution for 1 min and washed two times with distilled water for 2 min. Finally, sections were dehydrated in 95% and 100% ethanol, cleared in xylene, and mounted with a xylene-based mounting medium. The samples were examined using a Leica DMI6000B imaging system.

Immunofluorescence

Antigen retrieval was performed by transferring the rehydrated slides into pre-warmed (95C) sodium citrate buffer (10 mM Sodium citrate, 0.05% Tween 20, pH 6.0) for 30 min. Slides were allowed to cool to room temperature at least 20 min and washed twice for 5 min with distilled water. Then, slides were rinsed twice for 5 min with 1× PBS. Tissue sections were permeabilized with 0.1% Triton X-100 in 1× PBS for 45 min at room temperature and washed three times for 5 min with 1× PBS. Then, tissue sections were blocked for 1 hr in 5% goat serum at room temperature. For ZO-1 and E-cadherin dual staining, tissue sections were incubated with a rabbit anti-ZO-1 antibody (1:100) and mouse anti-E-cadherin antibody (1:100) in 5% goat serum overnight at 4C. The following day, tissue sections were warmed to room temperature for 20 min and washed three times for 5 min with 1× PBS. Tissue sections were incubated for 1 hr with their corresponding secondary antibodies (Alexa Fluor 488 conjugated goat anti-rabbit, Alexa Fluor 568 conjugated goat anti-mouse, 1:500) and then washed three times with 1× PBS. For nuclear staining, all slides were incubated with TO-PRO-3 iodide (1:1000) for 15 min and washed three times with 1× PBS. Then, samples were mounted under glass coverslips with ProLong Gold antifade reagent, and the edges of the coverslip were sealed with clear nail polish.

Confocal Laser Scanning Microscopy

The immunostained tissue sections were examined with a Carl Zeiss 700 LSM confocal microscope and ZEN software (Carl Zeiss, Thornwood, NY). All microscope settings were kept consistent for all samples. Exposure times of secondary antibody control images match their corresponding experimental images.

Adipocyte Quantification

For this study, we used five tissue sections per each SMG. The tile scanned bright-field images of SMG were captured at 10× optical magnification using a Leica DMI6000B inverted microscope. The diameter and percentage of adipocytes per each tissue section were calculated using ImageJ software. All statistical analyses were performed with GraphPad Prism 6. Data were analyzed by one-way analysis of variance (ANOVA) followed by pairwise post hoc Tukey's *t*-tests where $p < 0.001$ represents significant differences between experimental groups.

Results

Gamma Irradiation Causes Structural Alteration in Human SMG

As shown in Fig. 1A to F and Supplemental Fig. 1A and B, SMG from the 81-year-old female patient (non-irradiated, patient 1) as well as the 81-year-old male patient (non-irradiated, patient 2) displayed organized acinar and ductal structures (i.e., presence of aligned acinar and ductal cells surrounding lumens). We also observed a small inflammatory infiltrate, indicative of aging.[17,18] Conversely, SMG from the 65-year-old female patient (6 years 7 months post-irradiation, patient 3) displayed disorganized acinar and ductal structures (Fig. 1G–I, yellow arrow and Supplemental Fig. 1C). We also observed the presence of intralobular adipocytes (Supplemental Fig. 1C) and lymphocytic infiltration (Fig. 1I, red arrow). Similar to patient 4, SMG from the 39-year-old female patient (6 months post-irradiation, patient 4) displayed disorganized acinar and ductal structures (Fig. 1J–L, yellow arrow and Supplemental Fig. 1D), however, to a lesser degree than patient 3. Interestingly, the adipose tissue was observed mainly at the interlobular regions (Supplemental Fig. 1D), and lymphocyte infiltration also observed (Fig. 1L, red arrow).

Gamma Irradiation Causes Collagen Deposition in Human SMG

To further investigate collagen deposition in the different glands, we used Masson's Trichrome staining. As

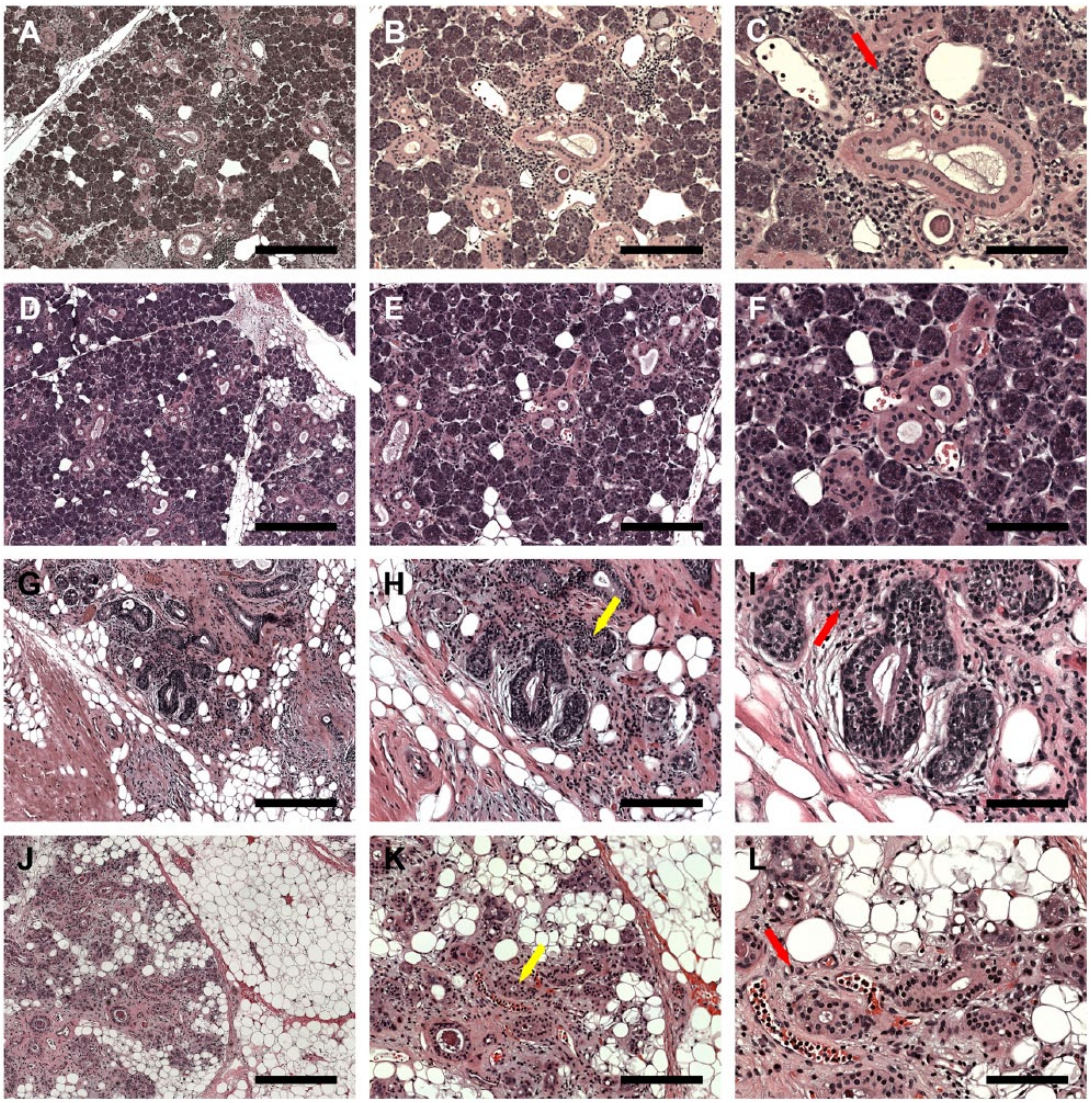

Figure 1. Hematoxylin and eosin (H&E)-stained histological sections of non-irradiated healthy (A–C, female; D–F, male), 6 years post-irradiated (G–I) and 6 months post-irradiated (J–L) head and neck cancer patients. H&E stain shows lymphocytic infiltration (red arrows) and disorganized ductal structures (yellow arrows). (A, D, G, J) Magnification 5×, bars = 400 μm; (B, E, H, K) magnification 10×, bars = 200 μm; (C, F, I, L) magnification 20×, bars = 100 μm.

shown in Fig. 2A to F and Supplemental Fig. 2A and B, SMG from the 81-year-old female patient (patient 1) and the 81-year-old male patient (patient 2) displayed low levels of collagen deposition (blue staining), which appears to be typical for the patient's age.[17,18] In contrast, SMG from the 65-year-old female patient (patient 3) displayed high collagen deposition levels in more than half of the gland, typical of long-term radiation exposure (see blue staining, Fig. 2G–I and Supplemental Fig. 2C).[19] Interestingly, SMG from the 39-year-old female patient (patient 4) displayed high levels of collagen deposition (although less than patient 3), which appears to be typical of early radiation stages[20] (see blue staining, Fig. 2J–L and Supplemental Fig. 2D).

Gamma Irradiation Causes Loss of Cell Junctions in Human SMG

To determine the degree of cell junction loss in the different glands, we used fluorescent staining. As shown in Fig. 3A to H, SMG from the 81-year-old female patient (patient 1) and the 81-year-old male patient (patient 2) displayed organized apical ZO-1 and basolateral E-cadherin. In addition, intact nuclear structures surrounded acinar and ductal lumens, typical of healthy

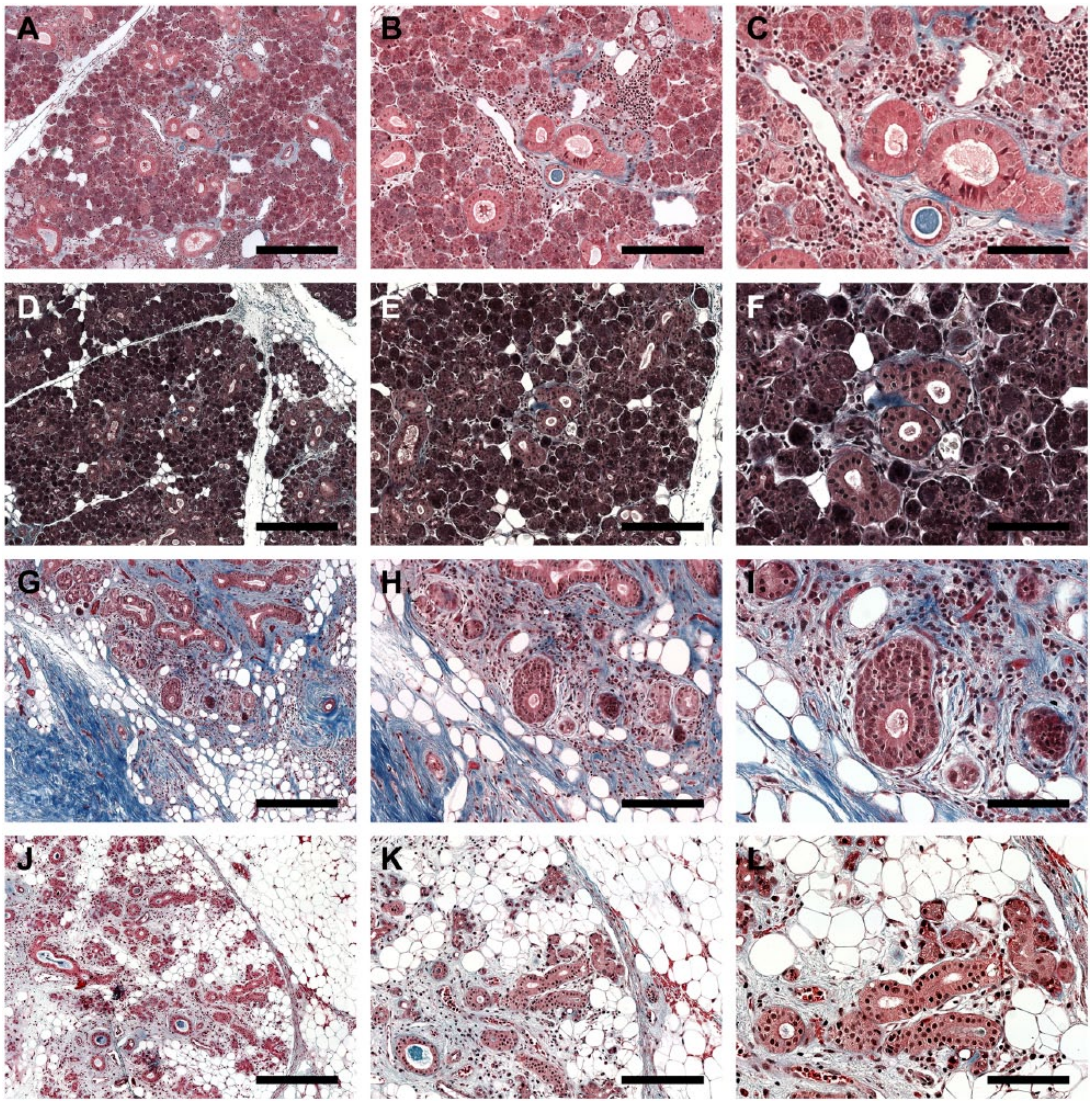

Figure 2. Masson's Trichrome stained histological sections of non-irradiated healthy (A–C, female; D–F, male), 6 years post-irradiated (G–I) and 6 months post-irradiated (J–L) head and neck cancer patients. Blue staining indicates the collagen deposition. (A, D, G, J) Magnification 5×, bars = 400 μm; (B, E, H, K) magnification 10×, bars = 200 μm; (C, F, I, L) magnification 20×, bars = 100 μm.

glands.[21] In contrast, SMG from the 65-year-old female patient (patient 3) showed disorganized nuclei and neither ZO-1 nor E-cadherin staining; however, we were able to see lumens (Fig. 3I–L, white arrows). Interestingly, SMG from the 39-year-old female patient (patient 4) displayed loss of ZO-1 staining but maintained organized basolateral E-cadherin (Fig. 3O) and presence of lumens (Fig. 3M–P, white arrows).

Gamma Irradiation Increases Adipocyte Numbers in Human SMG

To further investigate the presence of adipocytes in the irradiated tissues, we quantified the diameter and percentage of adipocytes using GraphPad Prism 6 and ImageJ software.[22,23] As shown in Figs. 4B and E, and 5A, SMG from the 81-year-old female patient (patient 1) and the 81-year-old male patient (patient 2) displayed a low percentage of adipocytes (patient 1: 4.35% ± 0.46%; patient 2: 7.62% ± 0.53%), typical for the patient's age.[18] In contrast, SMG from the 65-year-old female patient (patient 3) displayed a high percentage of adipocytes (22.32% ± 4.05%; Figs. 4H and 5A). SMG from the 39-year-old female patient (patient 4) displayed the highest percentage (36.33% ± 2.78%) of adipocytes (Figs 4K and 5A). The percentage of adipocytes was highly significant ($p < 0.001$). However, the percentage of adipocytes is not significantly different between the genders. In addition, the diameter of

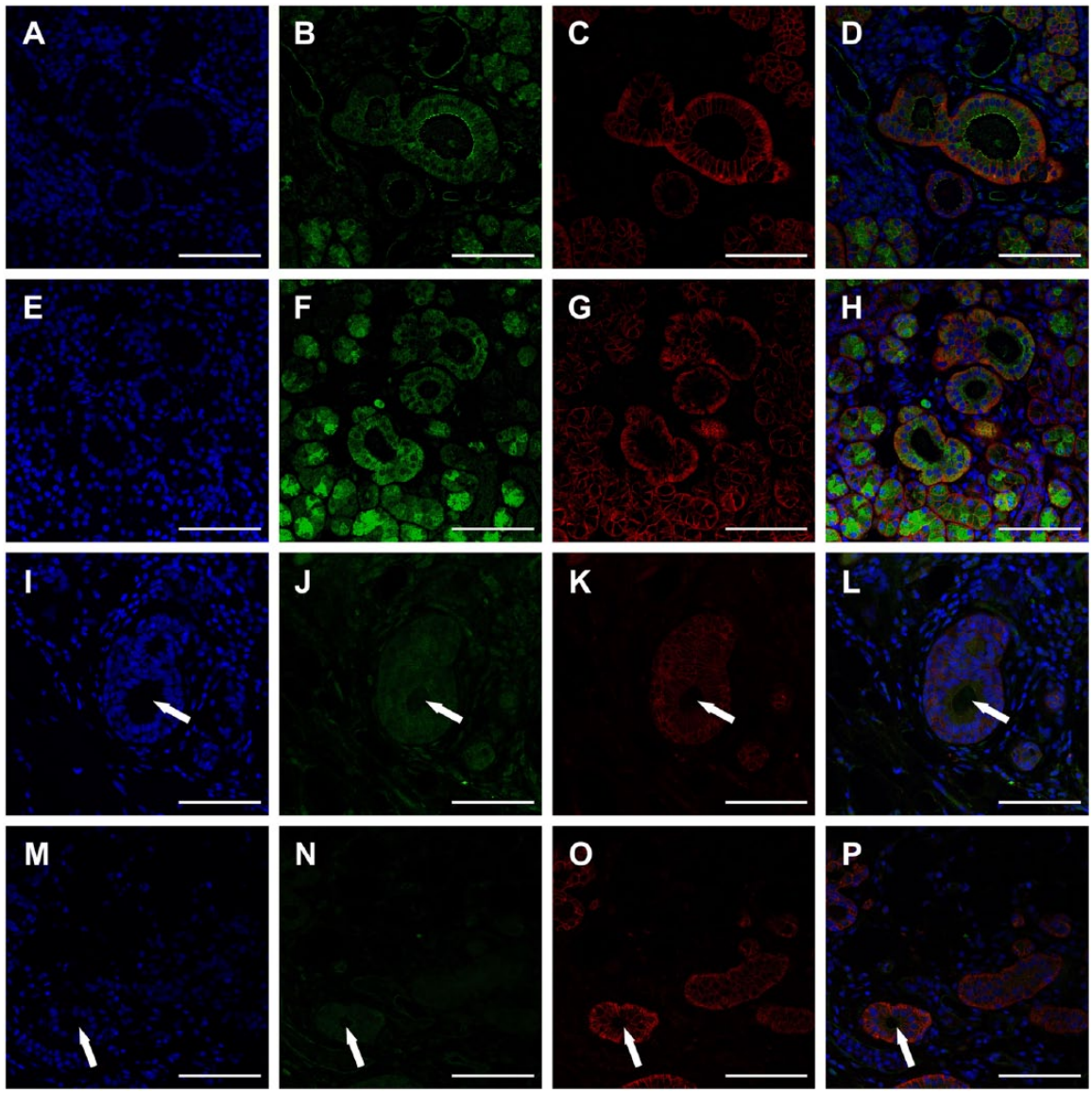

Figure 3. Zonula occludens-1 (ZO-1) and E-cadherin organization in non-irradiated healthy (A–D, female; E–H, male), 6 years post-irradiated (I–L) and 6 months post-irradiated (M–P) head and neck cancer patients. TO-PRO-3 iodide nucleic acid stain (A, E, I, M), ZO-1 (green; B, F, J, N), and E-cadherin (red; C, G, K, O). White arrows indicate lumens. Magnification 20×, bars = 100 μm.

adipocyte was not statistically significant difference between the groups ($p = 0.356$).

Discussion

Radiation treatment for head and neck cancer patients may result in oral side effects, which can reduce their quality of life.[5–9] Previous studies demonstrated that head and neck gamma irradiation significantly alters salivary gland structure and function. Particularly, there is loss of parenchymal tissue, acinar atrophy, dilated ducts, and fibrosis in major salivary glands.[24] Fibrosis is of particular interest, as it may limit function by reducing the innervation and irrigation of acinar and ductal structures. To investigate alteration of tissue structure after irradiation, we used SMG from two patients with very similar radiation doses (approximately 70 Gy). However, one subject (patient 3) was irradiated 6 years ago whereas the other subject (patient 4) was irradiated only 6 months ago. Results showed that patient 3 exhibited high levels of collagen while patient 4 displayed less collagen but more adipocytes when compared with patient 3. These results are consistent with previous studies indicating that fibrosis and collagen accumulation occurs as part of the post-irradiation wound

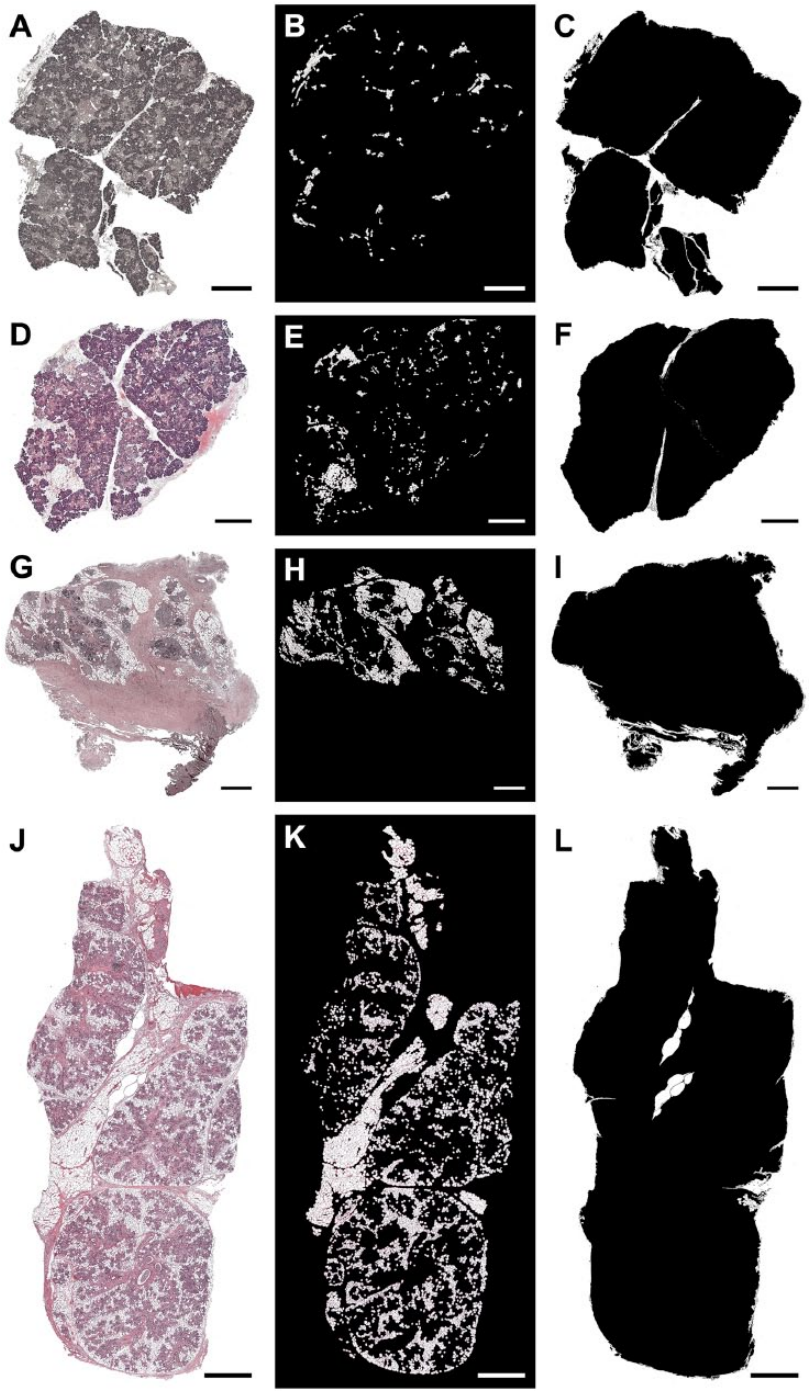

Figure 4. The presence of adipocytes in non-irradiated healthy (A–C, female; D–F, male), 6 years post-irradiated (G–I) and 6 months post-irradiated (J–L) head and neck cancer patients. Tiled images of SMG (hematoxylin and eosin [H&E] stain; A, D, G, J, magnification 10×, bars = 1 mm), adipocytes (B, E, H, K), and total tissue area (C, F, I, L) are shown.

healing process.[25] Furthermore, fibrosis in post-irradiated animals slowly increases over time.[26]

Regarding the number of adipocytes, we found that patient 3 had fewer adipocytes as compared with patient 4. In both cases, adipocytes were located within acinar and ductal structures, while in the healthy patient, adipocytes were located in the parenchymal region (as expected). Moreover, the total area of adipocytes in patient 4 was greater than in patient 3. These results suggest that the number of adipocytes,

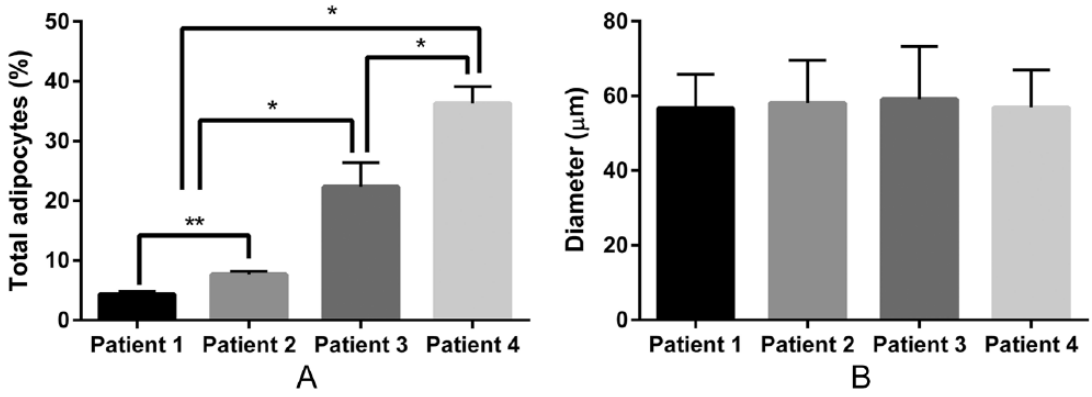

Figure 5. The percentage (A) and diameter (B) of adipocytes per each tissue section were calculated. Data represent the mean ± SD from five specimens per patient where asterisks indicate significant differences between experimental groups by an analysis of variance (ANOVA; *$p < 0.001$). However, the percentage of adipocytes is not significantly different between genders (**$p > 0.001$). The diameter of adipocytes is not significantly different between the four patients, $p = 0.356$.

as well as area, is higher right after irradiation and slowly decreases over time. Interestingly, it was previously reported that adipocyte size and number were significantly lower in post-irradiated mice when compared with healthy controls, while the size of adipocytes was not significantly altered in subcutaneous tissue.[27] However, these differences may be attributable to the different species and tissue location.

Adipose tissue is the most common tissue in the human body, and it plays an important role in numerous physiological processes. During adipocyte tissue expansion and differentiation, the extracellular matrix (ECM) requires remodeling to accommodate adipocytes; in turn, adipocytes secrete various peptides, cytokines, and complement factors. The most important change is the deposition of collagen at the cell–ECM border and biogenesis of the basement membrane. The function of adipose tissue is regulated by the interaction between cells and a variety of ECM proteins. The levels of type IV collagen, laminin, entactin, and glycosaminoglycans increase during the adipocyte tissue expansion and differentiation process. We are particularly interested in adipocytes as it has been previously reported that adipose tissue plays a role in wound healing by increasing angiogenesis while promoting tissue regeneration.[28] In addition, adipocytes have been shown to promote fibroblast migration into the wound.[29] Therefore, we could speculate that patient 3 had more fibroblasts and fewer adipocytes due to the wound healing process over time, while patient 4 may display early stages of the post-irradiation wound healing process. Consequently, we could propose that future clinical studies should be directed toward minimizing fibrosis by modulating adipocytes, as adipocytes cause collagen deposition.[29]

Regarding collagen deposition, it is known that when irradiation levels are low (≤40 ~ 50 Gy), a physiological wound healing process occurs.[30] For instance, large amounts of randomly oriented collagen are produced, then disorganized collagen is replaced with a more organized collagen during tissue remodeling.[31] However, after excessive radiation exposure, large amounts of collagen fibers replace the natural tissue, leading to loss of function. We observed high collagen deposition in SMG with a long post-irradiation time (see Table 1). In contrast, SMG with a short post-irradiation time (see Table 1) only showed a modest amount of collagen deposition. These results suggest that collagen deposition occurs over time after radiation exposure. Similar to other case studies, one limitation is the small sample size. Ideally, additional subjects would be analyzed over time to determine average rates of collagen deposition as a function of time and radiation dose. With such low subject numbers, individual heterogeneity in the healing response to radiation could equally be attributed for the differences noted. Once normative data are available, we could look at the individual variation in response to radiation therapy.

To prevent high amounts of post-irradiation collagen deposition, it would be important to study at what point collagen deposition becomes pathological. This could be accomplished by understanding the molecular composition of the collagen fibers post-irradiation. Changes in collagen deposition after irradiation cause the surrounding tissues to change. In fact, collagen levels induce tight junction phosphorylation and reorganization.[32] We observed loss of tight junction expression in post-irradiated SMG with a short post-irradiation time (Fig. 3N). In contrast, the adherens junction protein

E-cadherin was not only conserved but also maintained its basolateral localization (Fig. 3O). These results suggest that tight junctions may be one of the first structures to be altered in the post-irradiated glands. There are no previous studies showing alteration of tight junctions in the post-irradiated salivary glands. However, these proteins are critical for salivary gland function as they allow unidirectional fluid secretion as well as maintain a fence between apical and basolateral compartments for secretory function and need to be better understood.[33–35] A limitation of this study is that we only studied the scaffold protein, ZO-1, which links transmembrane tight junction proteins to the cytoskeleton.[36–39] Therefore, future studies including the transmembrane proteins (i.e., occludin, claudins, junctional adhesion molecules, ticellulin, and Coxsackie-adenovirus receptors) will be necessary to confirm that tight junction proteins are completely lost after irradiation of the glands. Head and neck irradiation causes structural alteration of SMGs. Our studies are consistent with previous studies showing collagen deposition after irradiation. However, this is the first study to demonstrate alteration of apico-basal polarity in post-irradiated salivary glands. In addition, there are no previous studies quantifying the amount and distribution of adipocytes under these conditions. These findings are an important first step in improving our understanding of the individual risk and variation in radiation-related salivary gland dysfunction.

Author Contributions

All authors have contributed to this article as follows: planning (KN, CLM, MMM, OJB), acquisition of samples (CLM, MMM, LB, JPH), execution of experiments (KN, BGT), analysis of data (KN, CLM, BGT, OJB), writing of manuscript (KN, CLM, OJB), and all authors have read and approved the manuscript as submitted.

Competing Interests

The authors declared no potential conflicts of interest with respect to the research, authorship, and/or publication of this article.

Funding

The authors disclosed receipt of the following financial support for the research, authorship, and/or publication of this article: This study is supported by the National Institutes of Health–National Institute of Dental and Craniofacial Research Grants R01DE022971 and R01DE021697 (to O.J.B.).

Literature Cited

1. Rischin D, Ferris RL, Le Q-T. Overview of advances in head and neck cancer. J Clin Oncol. 2015;33(29):3225–6.
2. American Cancer Society [Online]. Cancer Facts & Figures 2015. Available from: http://www.cancer.org/research/cancerfactsstatistics/cancerfactsfigures2015
3. Pulte D, Brenner H. Changes in survival in head and neck cancers in the late 20th and early 21st century: a period analysis. Oncologist. 2010;15(9):994–1001.
4. Suh Y, Amelio I, Guerrero Urbano T, Tavassoli M. Clinical update on cancer: molecular oncology of head and neck cancer. Cell Death Dis. 2014;5:e1018.
5. Jawad H, Hodson NA, Nixon PJ. A review of dental treatment of head and neck cancer patients, before, during and after radiotherapy: part 1. Br Dent J. 2015;218(2):65–8.
6. Monroe AT, Reddy SC, Gibbs GL, White GA, Peddada AV. Factors associated with radiation-induced nausea and vomiting in head and neck cancer patients treated with intensity modulated radiation therapy. Radiother Oncol. 2008;87(2):188–94.
7. Turner MD, Ship JA. Dry mouth and its effects on the oral health of elderly people. J Am Dent Assoc. 2007;138 Suppl 1:S15–20.
8. Kałużny J, Wierzbicka M, Nogala H, Milecki P, Kopeć T. Radiotherapy induced xerostomia: mechanisms, diagnostics, prevention and treatment—evidence based up to 2013. Otolaryngol Pol. 2014;68(1):1–14.
9. Lin C-Y, Ju S-S, Chia J-S, Chang C-H, Chang C-W, Chen M-H. Effects of radiotherapy on salivary gland function in patients with head and neck cancers. J Dent Sci. 2015;10(3):253–62.
10. Bjornstrom M, Axell T, Birkhed D. Comparison between saliva stimulants and saliva substitutes in patients with symptoms related to dry mouth. A multi-centre study. Swed Dent J. 1990;14(4):153–61.
11. Dost F, Farah CS. Stimulating the discussion on saliva substitutes: a clinical perspective. Aust Dent J. 2013;58(1):11–7.
12. Henson BS, Eisbruch A, D'Hondt E, Ship JA. Two-year longitudinal study of parotid salivary flow rates in head and neck cancer patients receiving unilateral neck parotid-sparing radiotherapy treatment. Oral Oncol. 1999;35(3):234–41.
13. Radfar L, Sirois DA. Structural and functional injury in minipig salivary glands following fractionated exposure to 70 Gy of ionizing radiation: an animal model for human radiation-induced salivary gland injury. Oral Surg Oral Med Oral Pathol Oral Radiol Endod. 2003;96(3):267–74.
14. Robar JL, Day A, Clancey J, Kelly R, Yewondwossen M, Hollenhorst H, Rajaraman M, Wilke D. Spatial and dosimetric variability of organs at risk in head-and-neck intensity-modulated radiotherapy. Int J Radiat Oncol Biol Phys. 2007;68(4):1121–30.
15. Ps SK, Balan A, Sankar A, Bose T. Radiation induced oral mucositis. Indian J Palliat Care. 2009;15(2):95–102.
16. Knox SM, Lombaert IM, Haddox CL, Abrams SR, Cotrim A, Wilson AJ, Hoffman MP. Parasympathetic stimulation improves epithelial organ regeneration. Nat Commun. 2013;4:1494.

17. De Wilde PC, Baak JP, van Houwelingen JC, Kater L, Slootweg PJ. Morphometric study of histological changes in sublabial salivary glands due to aging process. J Clin Pathol. 1986;39(4):406–17.
18. Dayan D, Vered M, Paz T, Buchner A. Aging of human palatal salivary glands: a histomorphometric study. Exp Gerontol. 2000;35(1):85–93.
19. Akita S. Treatment of radiation injury. Adv Wound Care. 2014;3(1):1–11.
20. Kojima T, Kanemaru S, Hirano S, Tateya I, Suehiro A, Kitani Y, Kishimoto Y, Ohno S, Nakamura T, Ito J. The protective efficacy of basic fibroblast growth factor in radiation-induced salivary gland dysfunction in mice. Laryngoscope. 2011;121(9):1870–5.
21. Mellas RE, Leigh NJ, Nelson JW, McCall AD, Baker OJ. Zonula occludens-1, occludin and E-cadherin expression and organization in salivary glands with Sjögren's syndrome. J Histochem Cytochem. 2015;63(1):45–56.
22. Parlee SD, Lentz SI, Mori H, MacDougald OA. Quantifying size and number of adipocytes in adipose tissue. Methods Enzymol. 2014;537:93–122.
23. Osman OS, Selway JL, Kępczyńska MA, Stocker CJ, O'Dowd JF, Cawthorne MA, Arch JR, Jassim S, Langlands K. A novel automated image analysis method for accurate adipocyte quantification. Adipocyte. 2013;2(3):160–4.
24. Cheng SCH, Wu VWC, Kwong DLW, Ying MTC. Assessment of post-radiotherapy salivary glands. Br J Radiol. 2011;84(1001):393–402.
25. Wynn TA, Ramalingam TR. Mechanisms of fibrosis: therapeutic translation for fibrotic disease. Nat Med. 2012;18(7):1028–40.
26. Gallet P, Phulpin B, Merlin J-L, Leroux A, Bravetti P, Mecellem H, Tran N, Dolivet G. Long-term alterations of cytokines and growth factors expression in irradiated tissues and relation with histological severity scoring. PLoS ONE. 2011;6(12):e29399.
27. Poglio S, Galvani S, Bour S, André M, Prunet-Marcassus B, Pénicaud L, Casteilla L, Cousin B. Adipose tissue sensitivity to radiation exposure. Am J Pathol. 2009;174(1):44–53.
28. Fu X, Fang L, Li H, Li X, Cheng B, Sheng Z. Adipose tissue extract enhances skin wound healing. Wound Repair Regen. 2007;15(4):540–8.
29. Schmidt BA, Horsley V. Intradermal adipocytes mediate fibroblast recruitment during skin wound healing. Development. 2013;140(7):1517–27.
30. Someya M, Sakata K, Nagakura H, Nakata K, Oouchi A, Hareyama M. The changes in irradiated salivary gland function of patients with head and neck tumors treated with radiotherapy. Jpn J Clin Oncol. 2003;33(7):336–40.
31. Madden JW, Peacock EE. Studies on the biology of collagen during wound healing. 3. Dynamic metabolism of scar collagen and remodeling of dermal wounds. Ann Surg. 1971;174(3):511–20.
32. Jaeger MM, Kalinec G, Dodane V, Kachar B. A collagen substrate enhances the sealing capacity of tight junctions of A6 cell monolayers. J Membr Biol. 1997;159(3):263–70.
33. Maria OM, Kim J-WM, Gerstenhaber JA, Baum BJ, Tran SD. Distribution of tight junction proteins in adult human salivary glands. J Histochem Cytochem. 2008;56(12):1093–8.
34. Kikuchi K, Kawedia J, Menon AG, Hand AR. The structure of tight junctions in mouse submandibular gland. Anat Rec. 2010;293(1):141–9.
35. Baker OJ. Current trends in salivary gland tight junctions. Tissue Barriers. 2016; 4(2): 1–14.
36. Shin K, Margolis B. ZOning out tight junctions. Cell. 2006;126(4):647–9.
37. Umeda K, Ikenouchi J, Katahira-Tayama S, Furuse K, Sasaki H, Nakayama M, Matsui T, Tsukita S, Furuse M, Tsukita S. ZO-1 and ZO-2 independently determine where claudins are polymerized in tight-junction strand formation. Cell. 2006;126(4):741–54.
38. Andreadis D, Epivatianos A, Mireas G, Nomikos A, Poulopoulos A, Yiotakis J, Barbatis C. Immunohistochemical detection of E-cadherin in certain types of salivary gland tumours. J Laryngol Otol. 2006;120(4):298–304.
39. Beavon IR. The E-cadherin-catenin complex in tumour metastasis: structure, function and regulation. Eur J Cancer. 2000;36(13):1607–20.